

Selective Inhibition of the Lactate Transporter MCT4 Reduces Growth of Invasive Bladder Cancer

Tilman Todenhöfer^{1,2}, Roland Seiler^{1,3}, Craig Stewart¹, Igor Moskalev¹, Jian Gao¹, Simroop Ladhar¹, Alireza Kamjabi¹, Nader Al Nakouzi¹, Tetsuharo Hayashi¹, Stephen Choi¹, Yuzhuo Wang¹, Sebastian Frees¹, Mads Daugaard¹, Htoo Zarni Oo¹, Pascale Fisel^{4,5}, Matthias Schwab^{4,6}, Elke Schaeffeler^{4,5}, James Douglas⁷, Jörg Hennenlotter², Jens Bedke², Ewan A. Gibb⁸, Ladan Fazli¹, Arnulf Stenzl², and Peter C. Black¹



Abstract

The significance of lactate transporters has been recognized in various cancer types, but their role in urothelial carcinoma remains mostly unknown. The aim of this study was to investigate the functional importance of the monocarboxylate transporter (MCT) 4 in preclinical models of urothelial carcinoma and to assess its relevance in patient tumors. The association of MCT4 expression with molecular subtypes and outcome was determined in The Cancer Genome Atlas (TCGA) cohort and two independent cohorts of patients with urothelial carcinoma. Silencing of MCT4 was performed using siRNAs in urothelial carcinoma cell lines. Effects of MCT4 inhibition on cell growth, apoptosis, and production of reactive oxygen species (ROS) were assessed. Moreover, effects on lactate efflux were determined. The *in vivo* effects of MCT4 silencing were assessed

in an orthotopic xenograft model. MCT4 expression was higher in the basal subtype. Decreased MCT4 methylation and increased RNA and protein expression were associated with worse overall survival (OS). Inhibition of MCT4 led to a reduction in cell growth, induction of apoptosis, and an increased synthesis of ROS. MCT4 inhibition resulted in intracellular accumulation of lactate. *In vivo*, stable knockdown of MCT4 reduced tumor growth. The expression of MCT4 in urothelial carcinoma is associated with features of aggressive tumor biology and portends a poor prognosis. Inhibition of MCT4 results in decreased tumor growth *in vitro* and *in vivo*. Targeting lactate metabolism via MCT4 therefore provides a promising therapeutic approach for invasive urothelial carcinoma, especially in the basal subtype. *Mol Cancer Ther*; 17(12); 2746–55. ©2018 AACR.

Introduction

Systemic therapy for advanced bladder cancer has evolved with the recent introduction of immune checkpoint inhibition. Although approximately half of patients respond to cisplatin-based chemotherapy, these responses are rarely durable (1). Checkpoint blockade is now established in the second-line setting, and the durability of response is much improved, but only approximately 20% of patients respond to treatment (2). As a result, patient outcomes remain poor, and novel therapies are still urgently needed. Recent data indicating that major

tumor-driven genomic aberrations induce transformations in cancer metabolism have led to a massive revival in the study of tumor metabolism in an effort to identify new therapeutic targets in cancer (3, 4).

It is well established that cancer cells reprogram their metabolism to process the majority of pyruvate by glycolysis, which is referred to as aerobic glycolysis or the Warburg effect (5). This adjustment of energy metabolism contributes significantly to uncontrolled cell proliferation and tumor growth. To eliminate the lactate that could accumulate in the intracellular compartment of highly glycolytic cancer cells, overexpression of selected monocarboxylate transporters (MCT) has been observed as common phenomenon in cancer cells.

Currently, there are 14 different members of the MCT protein family (6). MCT1 and MCT4 as well as their chaperone CD147 have been shown to be overexpressed in a variety of cancer types (7–17). Moreover, an association of these proteins with outcome has been identified in several tumors (9, 18–21). Epigenetic mechanisms have been shown to account for overexpression of MCTs. For example, expression of MCT4, encoded by the *SLC16A3* gene, has been shown to be significantly regulated by specific methylation in the promoter region of the *SLC16A3* gene in renal cell carcinoma (9, 21). Disruption of MCT1 or MCT4 in renal cell carcinoma, pancreatic cancer, and breast cancer has been shown to exert significant antitumor effects *in vivo* and *in vitro* by increased accumulation of intracellular lactate (22–24).

¹Vancouver Prostate Centre, University of British Columbia, Vancouver, Canada.

²Department of Urology, University Hospital, Tuebingen, Germany. ³Department of Urology, University of Bern, Bern, Switzerland. ⁴Dr. Margarete Fischer-Bosch-Institute of Clinical Pharmacology, Stuttgart, Germany. ⁵University of Tuebingen, Tuebingen, Germany. ⁶Departments of Clinical Pharmacology and Pharmacy and Biochemistry, University of Tuebingen, Tuebingen, Germany. ⁷Southampton General Hospital, Southampton, United Kingdom. ⁸GenomeDx Biosciences, Vancouver, Canada.

Note: Supplementary data for this article are available at Molecular Cancer Therapeutics Online (<http://mct.aacrjournals.org/>).

Corresponding Author: Peter C. Black, University of British Columbia, 2660 Oak Street, Vancouver, BC V6H 3Z6, Canada. Phone: 604-875-4818; Fax:604-875-5654; E-mail: pblack@mail.ubc.ca

doi: 10.1158/1535-7163.MCT-18-0107

©2018 American Association for Cancer Research.

Data on the role of MCT4 in urothelial carcinoma is limited (25–27). The aim of this study was to assess potential correlations of MCT4 expression in tumor samples with cancer-related outcome and evaluate the functional relevance of lactate export via MCT4 in preclinical models of urothelial carcinoma.

Patients and Methods

In silico analysis of TCGA data

The Urothelial Bladder Carcinoma (BLCA) cohort of TCGA included 412 patients. Clinical and gene expression (HTSeq – FPKM-UQ) data were downloaded from the Genomic Data Commons Portal (<https://portal.gdc.cancer.gov/>) on January 5, 2018. Gene expression data were transformed to $\log_2(\text{FPKM}+1)$ values for the analyses. Processed DNA methylation data were downloaded from <https://tga.xenahubs.net> on January 5, 2018. Statistical analyses were performed using R-3.3.2 (<https://www.r-project.org/>) including the additional packages `party_1.2-3` and `survival_2.41-3`. Median *SLC16A3* expression levels or median methylation levels at cg10183885, respectively, were used as cutoff for prediction of overall survival (OS). Log-rank *P* values were computed for the respective Kaplan–Meier curves. Univariate Cox proportional hazard regression models were applied to estimate HRs and 95% confidence intervals. Correlation analyses were performed using Spearman correlation tests. Information about TCGA and the investigators and institutions who constitute the TCGA research network can be found at <http://cancergenome.nih.gov/>.

The model based on classification to nearest centroids was used to assign the tumors to TCGA clusters as described previously (28).

Bladder cancer cohorts

For the first cohort (cohort A), we used radical cystectomy specimens from patients undergoing surgery for urothelial carcinoma between January 1996 and December 2006 at two academic centers (Vancouver General Hospital, Canada and University Hospital of Tuebingen, Germany). The American Joint Committee on Cancer (AJCC; 2002 Version) TNM classification was used for clinical and histopathologic staging (8).

For the second cohort (cohort B), pretreatment urothelial carcinoma tissue was collected at three institutions (University of Bern, Switzerland; Vancouver General Hospital, Canada; and University Hospital of Southampton, United Kingdom) from transurethral bladder tumor resection (TUR-BT) in patients who subsequently received at least three cycles of cisplatin-based neoadjuvant chemotherapy prior to radical cystectomy with pelvic lymph node dissection.

Tissue microarray and IHC

The TMA of cohort A included 691 cores from 180 patients undergoing radical cystectomy (437 cores of primary tumors, 181 cores from benign urothelium from tumor-free blocks, and 67 cores from lymph node metastases). The TMA of cohort B was constructed with 2 cores from each TURBT specimen ($n = 56$ from Bern and $n = 82$ from Vancouver/Southampton).

IHC staining was conducted by Ventana Autostainer Model Discover XT (Ventana Medical System) with enzyme-labeled biotin streptavidin system and solvent-resistant DAB Map kit using a 1/250 dilution of rabbit polyclonal antibody against MCT4 (SC-50329; Santa Cruz Biotechnology). Values on a four-point scale were assigned to each immunostaining. Descrip-

tively, 0 represented no staining by any tumor cells, 1 represented a faint or focal, questionably present stain, 2 represented a stain of convincing intensity in a minority of cells, and 3 a stain of convincing intensity in a majority of cells. In case of multiple cores available per patient, the maximum score was included in statistical analysis.

Microarrays

Gene expression microarray data were available from cohort B. Gene expression analysis was performed using GeneChip Human Exon 1.0 ST oligonucleotide microarrays (Affymetrix) according to the manufacturer's recommendations. RNA extraction and analysis were performed as described previously (28).

Cell lines and antibodies

A panel of human bladder cancer cell lines was provided by the Pathology Core of the Bladder Cancer SPORE at MD Anderson Cancer Center (RT4v6, RT112, UM-UC1, UM-UC5, UM-UC15, UM-UC6, UM-UC14, UM-UC16, 253JBV, T24, UM-UC3, and UM-UC13). For experiments in hypoxic conditions, an O₂ control glove box (Coy Laboratories) with 1% O₂ and 5% CO₂ at 37°C was used.

Western blot analysis/PCR

RNA extraction, qRT-PCR, protein extraction, and Western blots were performed as described previously (29). MCT4 (SC-50329, Santa Cruz Biotechnology) and Vinculin (ab18058, Abcam) antibodies were used in dilutions of 1:500 and 1:1,000. Primers and probes for MCT4 were purchased from Thermo Fisher Scientific (Hs00358829_m1). Actin B (Hs01060665_g1) served as reference gene.

RNA interference

For *in vitro* inhibition of MCT4, RNA interference was performed using siRNA and antisense oligonucleotides (ASO). Silencer select siRNAs (s17416 and s17417) and Silencer Select Negative Control #1 siRNA were purchased from Thermo Fisher Scientific. Transfection with ASO was performed as described previously using an MCT4-specific ASO (30). The sequence of the MCT4 ASO was 5'- T^{*}C^{*}C^{*}C^{*}A^{*}T^{*}G^{*}G^{*}C^{*}C^{*}A^{*}G^{*}G^{*}A^{*}G^{*}-G^{*}G^{*}T^{*}T^{*}G^{*}- 3' (* denotes the first-generation phosphorothioate backbone modification). As control, Scrambled B ASO was used (sequence: 5'- C^{*}C^{*}T^{*}T^{*}C^{*}C^{*}T^{*}C^{*}A^{*}A^{*}G^{*}C^{*}T^{*}T^{*}C^{*}C^{*}T^{*}C^{*}C^{*}-3'). Transfection was performed using Lipofectamine RNAiMAX (Life Technologies) for siRNA and Oligofectamine for ASO according to the manufacturer's protocol.

Cell proliferation and apoptosis

Cell proliferation was assessed in a 96-well plate by MTS assay (CellTiter 96 Aqueous One Solution Cell Proliferation Assay; Promega) according to the manufacturer's protocol. Assessment of apoptotic cells was performed using an Annexin V/7-Actinomycin (7-AAD) flow cytometry (FACS) assay (Becton Dickinson) according to the manufacturer's protocol.

Reactive oxygen species synthesis

For detection of reactive oxygen species (ROS), probes for a general oxidative stress indicator CM-H2DCFDA (Thermo Fisher Scientific) were used according to the manufacturer's protocol. CM-H2DCFDA is a chloromethyl derivative of 2',7'-dichlorodihydrofluorescein diacetate (H2DCFDA). Upon oxidation by ROS,

the nonfluorescent H2DCFDA is converted to the highly fluorescent 2',7'-dichlorofluorescein (DCF). CM-H2DCFDA exhibits much better retention in live cells than H2DCFDA.

Assessment of intra- and extracellular lactate levels

For lactate measurement, the BioVision (Milpitas) Colorimetric assay was used according to the manufacturer's protocol. To assess intracellular lactate levels, cells were resuspended in distilled water and disintegrated by vortexing.

Measurement of extracellular acidification rate and oxygen consumption rate

A Seahorse XF[®] Extracellular Flux Analyzer (Seahorse Bioscience) with the Seahorse Glycolysis Stress Kit was used for assessing the effect of MCT4 silencing on extracellular acidification rate (ECAR) and oxygen consumption rate (OCR). Optimal seeding densities and oligomycin (a strong inhibitor of ATP synthase used to prevent oxidative phosphorylation) concentrations were determined according to the Cell density and Oligomycin Optimization protocol of the manufacturer. Optimal seeding densities for T24, UC16, and UC13 were 2×10^4 cells per well. Optimal oligomycin concentration was 2.0 $\mu\text{mol/L}$. Preparation of cells and performance of the glycolysis stress assay was performed according to the manufacturer's protocol. The glycolysis stress kit is a standard method to assess important parameters of glycolysis by assessing extracellular acidification in different metabolic conditions. Whereas the addition of a saturating dose of glucose to cells cultured in glucose-free medium allows the analysis of the rate of glycolysis under basal conditions, the addition of oligomycin (leading to inhibition of mitochondrial ATP production) further shifts the energy production to glycolysis. This results in maximal glycolytic capacity and maximal lactate synthesis. This kit was used to assess differences in lactate efflux following MCT4 inhibition in different glycolytic conditions (basal conditions and maximal lactate synthesis).

In vivo knockdown of MCT4

All animal studies were approved by the Clinical Research Ethics Board of the University of British Columbia (Vancouver, British Columbia, Canada). To create a cell line with a stable knockdown for MCT4, UC16 cells were stably transfected with a commercially available shRNA from Santa Cruz Biotechnology targeting MCT4 (shMCT4) or a control vector shRNA (shCntrl) according to the manufacturer's protocol. A suspension of 5.0×10^4 UC16 cells transfected with shMCT4 ($n = 10$) or shCntrl ($n = 10$) in Matrigel (50 μL) was inoculated under the bladder mucosa in each of 20 six-week old male nude mice by percutaneous injection under ultrasound guidance as described previously (31). The tumor growth was monitored by ultrasound microimaging system Vevo770 (FUJIFILM VisualSonics). Tumor volumes were calculated using 3D imaging software according to the user manual.

Results

MCT4 expression is highest in basal bladder cancer and is associated with decreased OS

We first assessed the role of MCT4 expression in tumor samples from the TCGA (Supplementary Table S1), a separate cohort of chemotherapy-naïve patients (cohort A; Supplementary Table S2) and prior to chemotherapy in a cohort of patients

receiving neoadjuvant chemotherapy (cohort B; Supplementary Table S3).

Using the TCGA data, we observed a significant inverse correlation of degree of DNA methylation at selected CpG sites in the *SLC16A3* gene region (see Supplementary Table S4) and MCT4 mRNA expression. The most significant association was found for the CpG site cg10183885 ($R = -0.7$; $P < 0.0001$; Supplementary Fig. S1). In cohort B both protein and gene expression data were available, and here a significant correlation of gene expression and protein expression was observed (Supplementary Fig. S2).

We next compared the expression of MCT4 in benign urothelium and cancer tissue using IHC in our cohort of chemotherapy-naïve patients (cohort A). MCT4 protein expression was observed in the membrane of the cancer cells. Independent of the cancer cell expression, it was more diffusely expressed in the stromal compartment. In CD8⁺ T cells, MCT4 expression was observed in the cytoplasm with enhanced perinuclear staining and occasional nuclear localization (Supplementary Fig. S3). We observed a significantly higher expression of MCT4 in primary tumors compared with benign urothelium (Supplementary Fig. S4). No correlation with tumor stage or lymph node involvement was observed (Supplementary Fig. S5).

Specific molecular subtypes of bladder cancer with distinct biological features have been introduced on the basis of mRNA expression profiles. Using the molecular subtypes introduced by the TCGA, we observed a significant overexpression of MCT4 mRNA in the TCGA clusters 3 and 4 (basal subtype) both in the TCGA cohort (Fig. 1A) and our own cohort (cohort B; Fig. 1B). The overexpression of MCT4 mRNA in basal tumors was also observed when using clustering from the most recent updated analysis of the entire TCGA cohort (Supplementary Fig. S6; ref. 32). Furthermore, in cohort B a higher MCT4 protein expression (Fig. 1C) was observed in clusters 3 and 4, but no MCT4 protein expression data were available from the TCGA. Representative staining patterns of MCT4 protein expression are shown in Fig. 1E. Of note, DNA methylation at cg10183885 in the *SLC16A3* gene region also correlated significantly with molecular subtypes in the TCGA cohort, with lower methylation in basal (clusters 3 and 4) compared with luminal tumors (clusters 1 and 2; Fig. 1D).

In the TCGA cohort, high MCT4 gene expression and low DNA methylation at cg10183885 were associated with inferior OS (Fig. 2A and B, respectively). In our own cohort of chemotherapy-naïve patients undergoing cystectomy (cohort A), high MCT4 protein expression (Fig. 2C) was associated with inferior OS. In patients receiving neoadjuvant chemotherapy (cohort B), MCT4 gene (Supplementary Fig. S7) and protein expression (Fig. 2D) showed no association with outcome.

Inhibition of MCT4 reduced bladder cancer cell growth *in vitro*

Expression of MCT4 protein was detected in 7 of 12 cell lines (Supplementary Fig. S8A). The two cell lines with highest expression were T24 and UC13. This was strongly concordant with results from qRT-PCR for MCT4 expression showing low or no expression in 5 of 12 cell lines and highest expression in T24 and UC13 (Supplementary Fig. S8B).

We selected three MCT4-positive cell lines (T24, UC16, UC13) for MCT4-inhibition using RNA interference. Successful inhibition of MCT4 following siRNA transfection was observed in all cell lines (Fig. 3A and B).

MCT4 inhibition led to a significant decrease of cell growth in all MCT4-positive cell lines in normoxic (Fig. 3C–E) and hypoxic

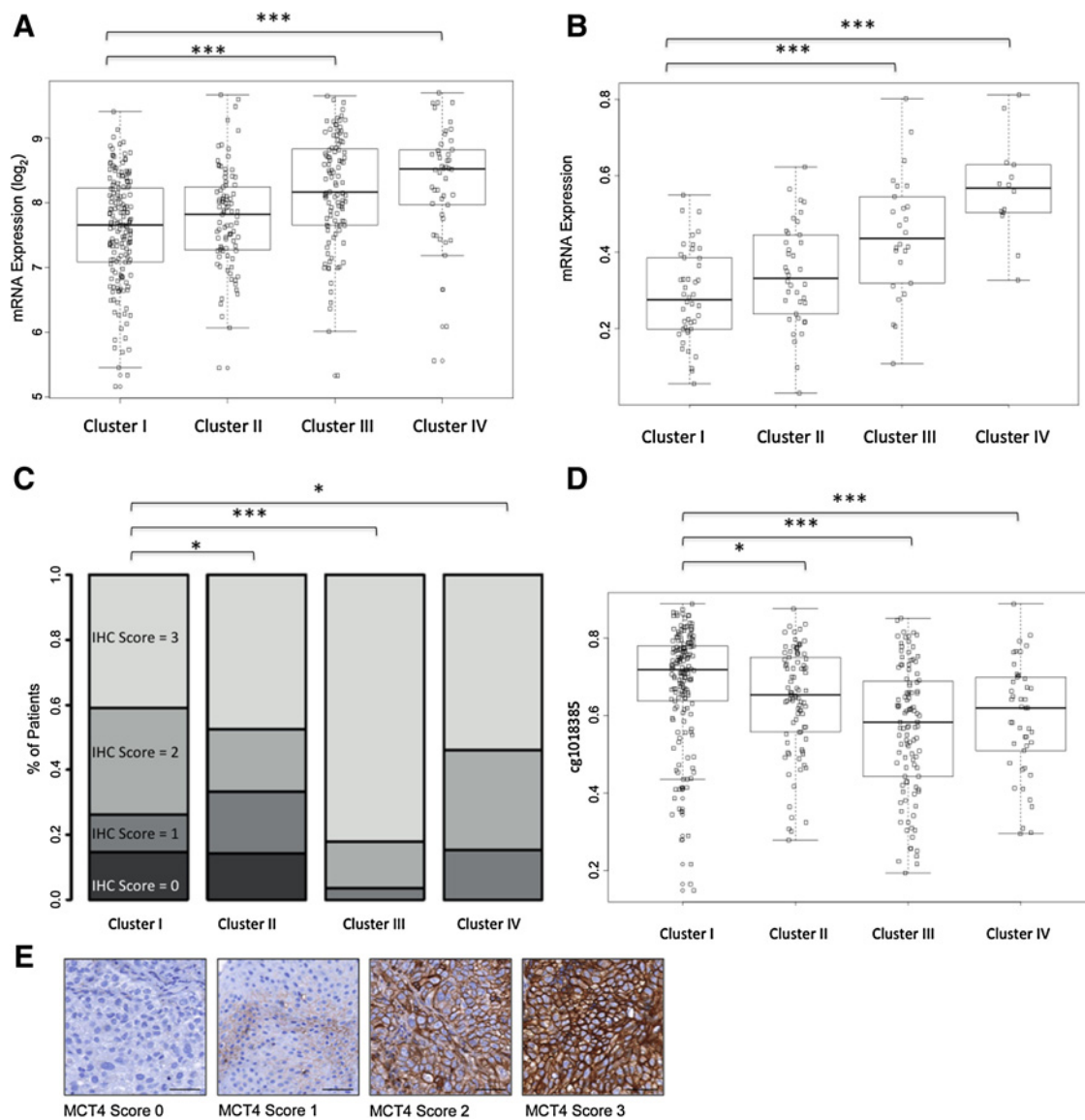
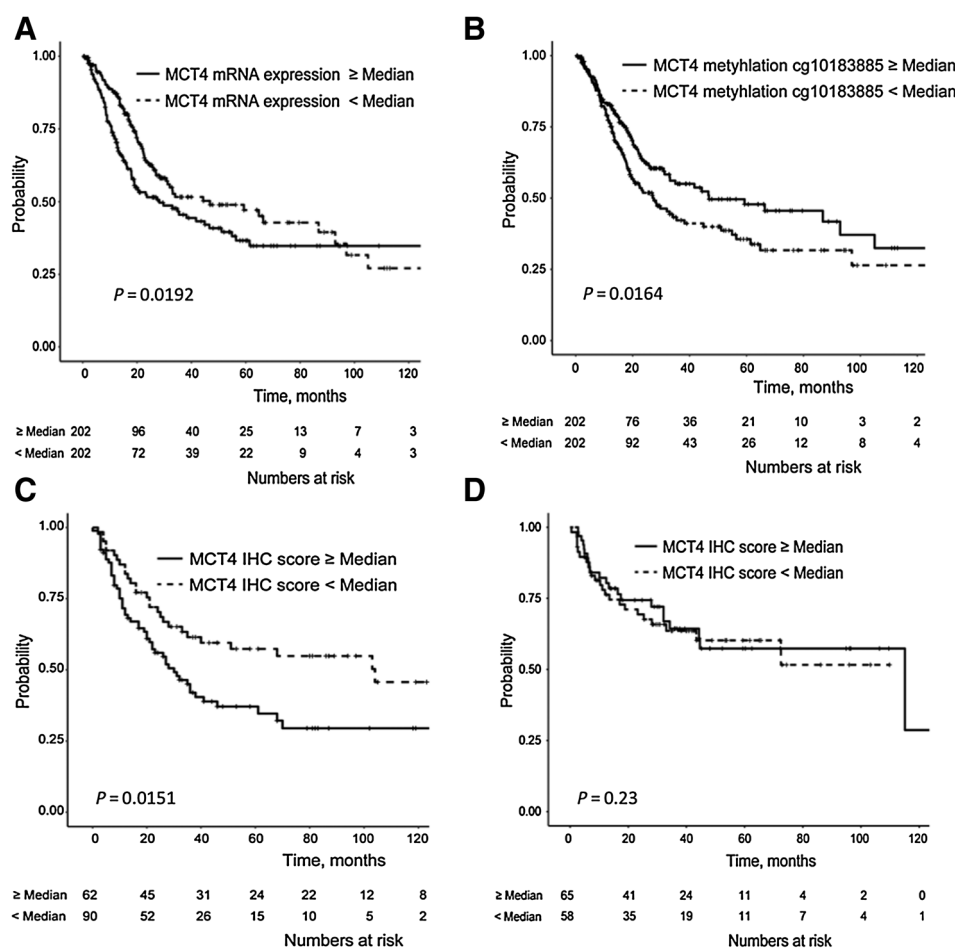


Figure 1. Correlation of molecular subtypes with MCT4 gene methylation, gene and protein expression. Expression differences were analyzed using Cluster I as reference. **A**, MCT4 mRNA expression correlates with molecular subtypes in the TCGA cohort ($n = 408$). **B**, MCT4 gene expression correlates with molecular subtypes in a cohort of patients receiving neoadjuvant chemotherapy (cohort B; $n = 147$). **C**, MCT4 protein expression correlates with molecular subtypes in a cohort of patients receiving neoadjuvant chemotherapy (cohort B; $n = 147$). **D**, DNA methylation at cg1018385 in the *SLC7A3* gene region correlates with molecular subtypes in the TCGA cohort. **E**, Representative staining patterns for applied staining scores using IHC. *, $P < 0.05$; **, $P < 0.01$; ***, $P < 0.001$.

conditions (Supplementary Fig. S9). Hypoxia was used to augment MCT4 expression and activity with the intention of accentuating the effects of MCT inhibition (33). Transfection of a MCT4-negative cell line (RT4) with siRNA targeting MCT4 did not affect cell growth (Supplementary Fig. S10). Next, we assessed whether deprivation of glucose, an important substrate for lactate synthesis, which has been shown to attenuate the effect of MCT4 inhibition in other cancers (23), may influence the effect of MCT4 silencing on cell growth in normoxic and hypoxic conditions (Supplementary Fig. S11). A difference in cell growth of cells transfected with siRNAs for

MCT4 versus control siRNAs was only observed for T24 when culturing the cells in hypoxic and glucose-deprived conditions, although the impact was less than in normal glucose conditions (Supplementary Fig. S11). In contrast, siRNAs for MCT4 no longer influenced the growth of UC16 and UC13 when grown in glucose-deprived conditions indicating that the mechanism leading to cell growth reduction in cells with decreased MCT4 inhibition is partially dependent of glucose levels (Supplementary Fig. S11). To confirm that effects of MCT4 inhibition on growth of breast cancer cells are not dependent on the mechanism of RNA interference, we used MCT4-specific ASOs.

**Figure 2.**

Correlation of MCT4 characterization with urothelial carcinoma patient outcome. **A**, MCT4 gene expression correlates with poor OS in the TCGA dataset. **B**, DNA methylation at cg10183885 correlates with OS in the TCGA dataset. **C**, MCT4 protein expression correlates with poor OS in patients not treated with neoadjuvant chemotherapy (cohort A). **D**, MCT4 protein expression does not correlate with outcome in patients receiving neoadjuvant chemotherapy (cohort B).

Dose-dependent inhibition of cell growth was confirmed using different concentrations of the ASO (Supplementary Fig. S12).

Antiproliferative effects of MCT4 inhibition were associated with increased apoptosis, accumulation of ROS, and impaired lactate efflux

Previous data in other tumor types suggest that MCT4 inhibition induces apoptosis by altering levels of ROS (24). Following MCT4 inhibition via siRNA, a significant increase in apoptotic cells was observed using Annexin FACS (Fig. 4A). This was associated with a significant increase in concentrations of ROS (Fig. 4B).

To determine the functional consequence of MCT4 inhibition on lactate efflux, we analyzed intra- and extracellular lactate concentrations after MCT4 silencing (Fig. 4C and D). In all three cell lines, a significant increase in intracellular lactate was observed, whereas extracellular lactate concentrations were significantly lower in MCT4-silenced cells compared with cells transfected with control siRNAs (Fig. 4C and D).

The impact of impaired lactate efflux on downstream metabolism after MCT inhibition was tested with the Glycolysis Stress Kit on the Seahorse Analyzer. Transfection of bladder cancer cells with siRNA against MCT4 led to an attenuated extracellular acidification following injection of glucose (Fig. 4E) and oligomycin (Fig. 4F) confirming reduced lactate efflux due to MCT4

inhibition. MCT4 silencing led to a modest but nonsignificant increase in OCRs in baseline conditions and before oligomycin injection (Supplementary Fig. S13A–S13C).

MCT4 inhibition reduces growth of orthotopic bladder cancer xenografts

Following our observation that MCT4 inhibition reduces cell growth *in vitro*, we established a cell line with stable knockdown of MCT4 using shRNA to investigate the effect of MCT4 inhibition on *in vivo* tumor growth, (Fig. 5A and B). We observed a significant inhibition of tumor growth in cells with MCT4 inhibition compared with cells transfected with mock shRNA (Fig. 5C).

Discussion

MCT4 has been shown in several solid tumor types to be essential for adaptation to tumor-specific metabolic processes, as well as being important for tumor growth. The inhibition of tumor metabolic processes has shown promising effects in pre-clinical studies of some of these solid tumors. Here, we present one of the first reports describing a correlation between MCT4 expression and adverse outcomes in patients with urothelial carcinoma. We have also demonstrated *in vitro* a key functional role for MCT4 in urothelial carcinoma metabolism. Knockdown of MCT4 using both siRNA and an ASO led to a significant growth

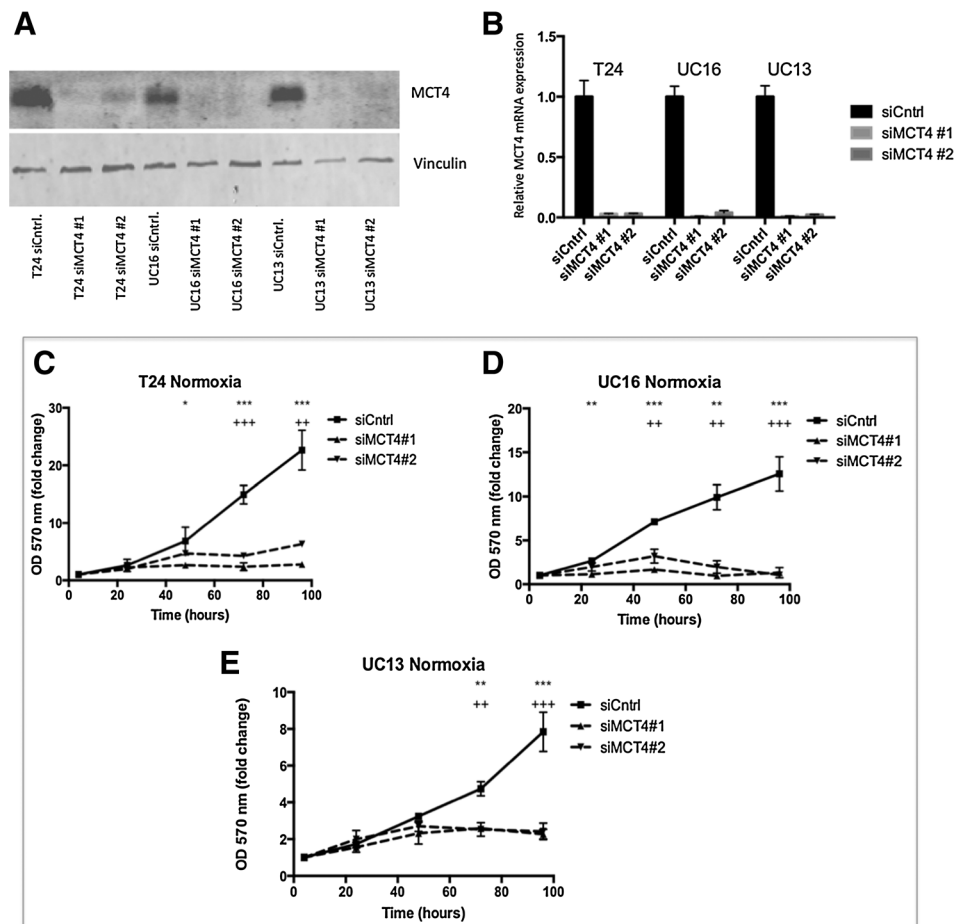


Figure 3.

Use of RNA interference to inhibit MCT4 expression in urothelial carcinoma cell lines. **A**, MCT4 protein expression in T24, UC16, and UC13 cells after transfection with control siRNA (siControl) or siRNA for MCT4 (siMCT4 #1, siMCT4 #2). **B**, MCT4 gene expression in T24, UC16, and UC13 cells after transfection with control siRNA (siControl) or siRNA for MCT4 (siMCT4 #1, siMCT4 #2). **C–E**, Effect of MCT4 gene silencing on cell growth in T24 (**C**), UC16 (**D**), and UC13 (**E**) cells in normoxic conditions.

P values siMCT4#1 versus. siCntrl: *, < 0.05; **, < 0.01; ***, < 0.001
P values siMCT4#2 versus. siCntrl: + < 0.05 ++ < 0.01 +++ < 0.001.

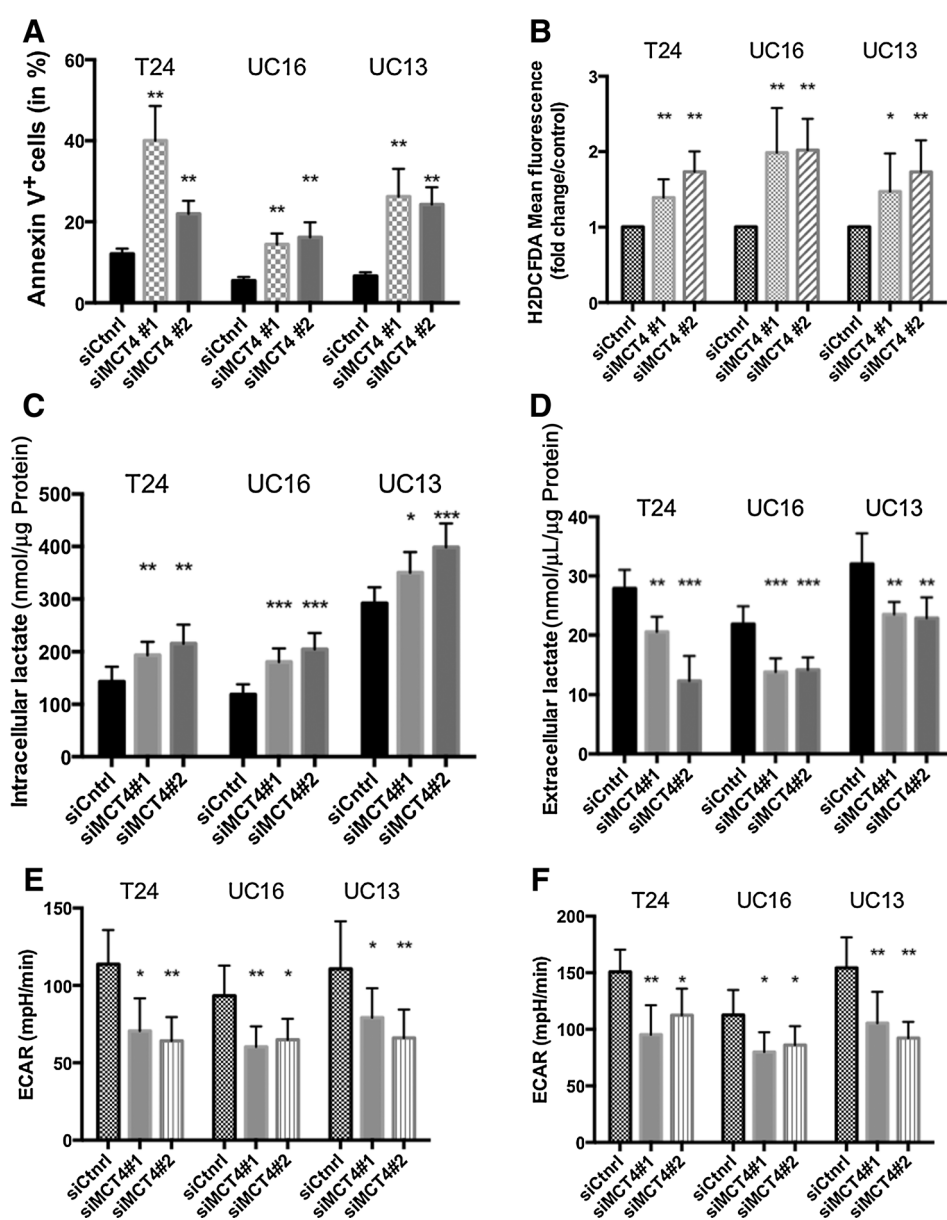
reduction in cell lines expressing MCT4. Consistent with this data, we also observed a significant growth reduction after stable silencing of MCT4 in an orthotopic xenograft model.

The expression pattern of MCT4 in patient tumors suggests potential clinical relevance of our findings. We observed that MCT4 expression is increased in urothelial carcinoma tissue compared with benign urothelium and that it predicts poor OS. High MCT4 expression by IHC predicted poor outcome also in a separate study of 360 patients with different stages of urothelial carcinoma (27). Neither this study nor our own revealed a correlation of MCT4 expression with tumor stage or lymph node involvement. We observed furthermore that MCT4 expression is associated with the basal urothelial carcinoma subtype. Basal tumors have been shown to exhibit features of aggressive tumor growth and poor outcome. An association of basal tumors with expression of lactate transporters and other proteins present in highly glycolytic tumor cells has been also observed in breast cancer (34). Moreover, patients with basal urothelial carcinoma seem to derive significant benefit from neoadjuvant chemotherapy (28). Although it remains to be elucidated whether the expression of MCT4 is a predictor of response to chemotherapy, our data suggest preliminarily that the prognostic significance of MCT4 differs between patients treated with and without neoadjuvant chemotherapy. Patients with high expression of MCT4 showed poor OS if treated by RC alone, whereas MCT4 expression

did not correlate with outcome of patients receiving neoadjuvant chemotherapy.

Using the TCGA dataset, we observed that the expression of MCT4 was significantly dependent of the degree of DNA methylation at a specific CpG site in the *SLC16A3* gene region (cg10183885) and that patients with increased methylation have a favorable outcome. Previously published methylation data on site cg10183885 support a correlation of methylation with MCT4 expression in breast cancer cell lines (35). This is in accordance with previous studies showing that methylation of specific CpG sites in the *SLC16A3* gene region is an important regulator of gene expression and directly correlates with outcome of patients with renal cell carcinoma (9).

The mechanism behind reduced cell growth after MCT4 inhibition remains to be elucidated. This antiproliferative effect was observed in normoxic as well as hypoxic conditions, even though MCT4 expression is known to increase in hypoxia (33). The effect of MCT4 disruption was strongly attenuated in glucose-deprived conditions, indicating a strong dependence on glucose availability. Both by direct measurement of intra- and extracellular lactate and determination of the ECAR, a significant disruption of lactate efflux was observed. Previous studies suggested that MCT4 inhibition causes a metabolic switch to more oxygen-consuming processes that result in increased production of ROS. This in turn leads to increased apoptosis (24). We observed an increased

**Figure 4.**

Effect of MCT4 inhibition on apoptosis and lactate efflux. **A**, Effect of MCT4 siRNA transfection on apoptosis assessed by annexin V flow cytometry (FACS). **B**, Effect of MCT4 silencing on synthesis of ROS assessed by FACS for the ROS indicator CM-H2DCFDA (chloromethyl derivative of 2',7'-dichlorodihydrofluorescein diacetate). Relative changes of mean CM-H2DCFDA fluorescence compared with controls are presented. **C** and **D**, Effect of gene expression silencing of MCT4 on intra- (**C**) and extracellular (**D**) lactate levels. **E**, Extracellular acidification after addition of glucose (**E**) and oligomycin (**F**; *, $P < 0.05$; **, $P < 0.01$; ***, $P < 0.001$).

production of ROS in cells with disrupted MCT4 expression, but OCRs were not consistently elevated. Figure 6A and B provides a potential mechanism by which MCT4 inhibition leads to cell death in breast cancer cells. However, we have not proved all components of this model in this study, such as the resultant increase in oxidative phosphorylation.

The antineoplastic activity of MCT4 inhibition is assumed to be mainly a result of lactate accumulation in the cell, subsequent inhibition of glycolysis, and an intracellular acidification. In this context, it is critical to consider to what extent the blockade of a pH-regulating protein such as MCT4 is sufficient to overcome compensatory mechanisms induced by other pH-regulating proteins (36). These proteins include the Na^+/H^+ exchanger NHE1, carbonic anhydrases such as CAIX and CAXII, and HCO_3^- transporters (37, 38). These proteins interact directly with MCTs. For

example, extrusion of lactate via MCTs can be enhanced by the activity of carbonic anhydrases (39). The critical intracellular pH value required to induce cell death by any intervention inhibiting these pH-regulating mechanisms remains unknown, although an intracellular pH of 6.0 has been proposed (36, 37). To achieve a significant reduction of intracellular pH in tumor cells, which are thought to have a more alkaline intracellular pH than benign cells, the movement of membrane-permeant weak acids and permeant forms of lactate have to be taken into account. By inhibiting lactate transporters and H^+ efflux mediated by other proteins, the consecutive decrease of intracellular pH is likely to promote the movement of permeant weak acids and permeant forms of lactate (36). Overcoming such compensatory mechanisms is a major challenge for approaches targeting mechanisms that regulate the intracellular

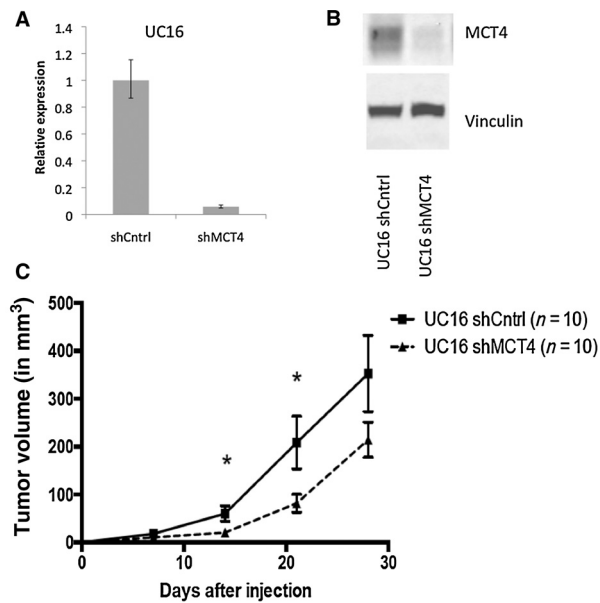


Figure 5. Effect of MCT4 inhibition using shRNA on *in vivo* tumor growth using an orthotopic xenograft model. **A** and **B**, MCT4 gene and protein expression following stable transfection with control shRNA (shCntrl) or shRNA for MCT4 (shMCT4). **C**, Tumor growth in nude mice after implantation of shCntrl and shMCT4 UC16 cells assessed by three-dimensional ultrasonography (*, $P < 0.05$; **, $P < 0.01$; ***, $P < 0.001$).

pH. Combined modulation of more than one mechanism may enhance the effects of metabolic inhibitors.

Both our tumor tissue and preclinical analyses have inherent limitations. We used normal appearing urothelium from patients with bladder cancer undergoing cystectomy as representative of benign urothelium. We cannot rule out that MCT4 expression in the urothelium of noncancer bearing bladders might differ from the pattern we observed in this study. These tissue studies are also limited by their retrospective nature. Furthermore, *in vitro* and xenograft models for the assessment of functional silencing of MCT4 are not able to represent the full complexity of muscle invasive urothelial carcinoma. Especially the interaction with the tumor microenvironment and the host immune system cannot be assessed by these models. Recently, MCT4 expression in cancer-surrounding fibroblasts has been shown to be an important promoter of tumor growth (26). Although the functional changes we have observed in MCT4-silenced cells are consistent with previously reported studies in this domain, our study cannot provide a detailed mechanism by which the changes in lactate metabolism induce apoptosis. This limitation also applies to previous studies investigating the potential inhibition of metabolic processes as a therapeutic strategy in cancer therapy (23, 24, 40). The main link between glucose metabolism, pH regulation, and cell cycle and cell death is an area of active investigation (36). We did not perform overexpression experiments to address whether this would result in opposing effects compared with inhibition. Our xenograft model does not allow us to study metastasis, because the local growth of tumor leads to the demise of the mice before the tumors metastasize.

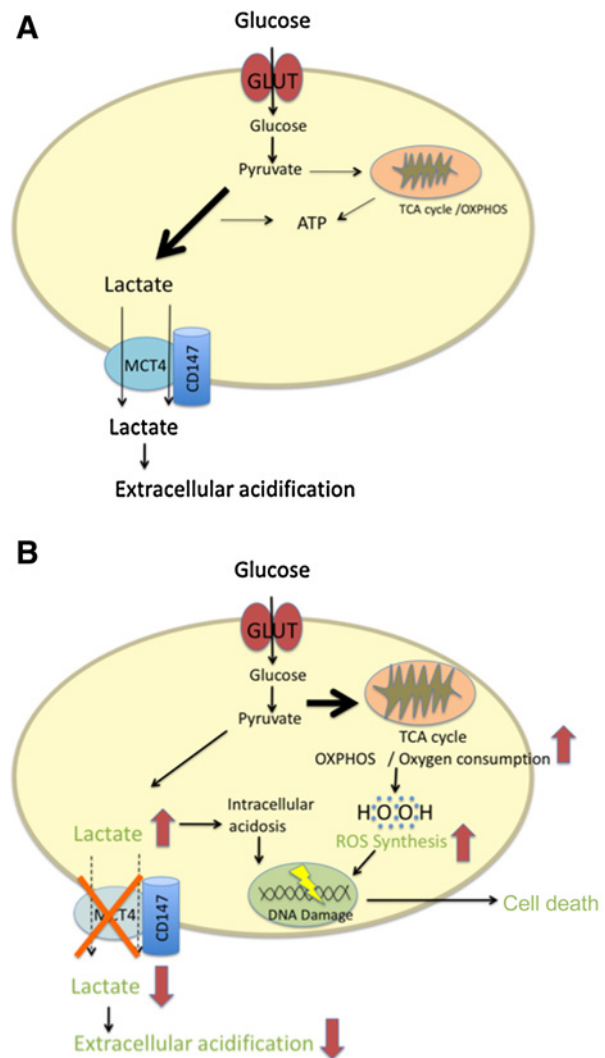


Figure 6. Schematic model of potential influence of MCT4 inhibition on cell metabolism in urothelial carcinoma. **A**, Green font indicates that this component of the model is supported by data of this study in cells with intact MCT4—a high proportion of pyruvate is metabolized to lactate. Monocarboxylate transporters (including MCT4) mediate lactate efflux to prevent intracellular acidosis. **B**, Inhibition of MCT4 expression leads to intracellular accumulation of lactate. In parallel, increased levels of ROS can be found potentially as a result of increased flux of pyruvate into tricarboxylic acid cycle (TCA) with subsequent oxidative phosphorylation (OXPHOS) and oxygen consumption. Increased lactate and ROS levels promote cell death.

Conclusions

In conclusion, our study shows that MCT4 expression in invasive urothelial carcinoma correlates with aggressive tumor biology and poor outcome. Moreover, inhibition of MCT4 demonstrates considerable antineoplastic effects both in preclinical models of urothelial carcinoma. Therefore, targeting MCT4 may represent a promising approach for treatment of urothelial carcinoma.

Disclosure of Potential Conflicts of Interest

T. Todenhöfer is a consultant/advisory board member for Amgen, MSD, and Roche. S. Choi has ownership interest in MCT4 ASO Patent. A. Stenzl has received Speakers' Bureau Honoraria from Janssen, Ipsen Pharma, Sanofi Aventis, CureVac, and Astellas and is a consultant/advisory board member for Ipsen Pharma GmbH, Roche, Janssen, Alere, Bristol-Myers-Squibb, Stebabiotec, and Syngro. No potential conflicts of interest were disclosed by the other authors.

Authors' Contributions

Conception and design: T. Todenhöfer, Y. Wang, P.C. Black

Development of methodology: T. Todenhöfer, N. Al Nakouzi, P.C. Black

Acquisition of data (provided animals, acquired and managed patients, provided facilities, etc.): T. Todenhöfer, R. Seiler, C. Stewart, I. Moskalev, J. Gao, A. Kamjabi, S. Frees, H.Z. Oo, J. Douglas, J. Hennenlotter, J. Bedke, A. Stenzl, P.C. Black

Analysis and interpretation of data (e.g., statistical analysis, biostatistics, computational analysis): T. Todenhöfer, R. Seiler, C. Stewart, N. Al Nakouzi, H.Z. Oo, P. Fisel, M. Schwab, E. Schaeffeler, E.A. Gibb, P.C. Black

Writing, review, and/or revision of the manuscript: T. Todenhöfer, R. Seiler, C. Stewart, Y. Wang, M. Daugaard, H.Z. Oo, P. Fisel, M. Schwab, E. Schaeffeler, J. Hennenlotter, J. Bedke, A. Stenzl, P.C. Black

Administrative, technical, or material support (i.e., reporting or organizing data, constructing databases): C. Stewart, T. Hayashi, S. Choi, S. Frees, J. Hennenlotter

Study supervision: T. Todenhöfer, Y. Wang, P.C. Black

Others (research assistant; running experiments under the guidance of postdoctoral supervisor): S. Ladhari

Other (pathology): L. Fazli

Acknowledgments

The results shown here are in part based upon data generated by the TCGA Research Network. We would like to thank The Cancer Genome Atlas initiative, all tissue donors, and investigators who contributed to the acquisition and analyses of the samples used in this study. This study was supported by the German Cancer Foundation (grant no. 111282, to T. Todenhöfer). P. Black was supported by the Canadian Cancer Research Society Research Institute (grant no. 704108) and the Khosrowshahi Family Research Fund. P. Fisel, M. Schwab, and E. Schaeffeler were supported by the Robert Bosch Stiftung, Stuttgart, Germany and the German Cancer Consortium (DKTK) and German Cancer Research Center (DKFZ), Heidelberg, Germany.

The costs of publication of this article were defrayed in part by the payment of page charges. This article must therefore be hereby marked *advertisement* in accordance with 18 U.S.C. Section 1734 solely to indicate this fact.

Received February 7, 2018; revised July 16, 2018; accepted September 20, 2018; published first September 27, 2018.

References

- von der Maase H, Sengelov L, Roberts JT, Ricci S, Dogliotti L, Oliver T, et al. Long-term survival results of a randomized trial comparing gemcitabine plus cisplatin, with methotrexate, vinblastine, doxorubicin, plus cisplatin in patients with bladder cancer. *J Clin Oncol* 2005;23:4602–8.
- Bellmunt J, de Wit R, Vaughn DJ, Fradet Y, Lee JL, Fong L, et al. Pembrolizumab as second-line therapy for advanced urothelial carcinoma. *N Engl J Med* 2017;376:1015–26.
- Cairns RA, Harris IS, Mak TW. Regulation of cancer cell metabolism. *Nat Rev Cancer* 2011;11:85–95.
- Adekola K, Rosen ST, Shanmugam M. Glucose transporters in cancer metabolism. *Curr Opin Oncol* 2012;24:650–4.
- Warburg O, Wind F, Negelein E. The metabolism of tumors in the body. *J Gen Physiol* 1927;8:519–30.
- Halestrap AP. Monocarboxylic acid transport. *Compr Physiol* 2013;3:1611–43.
- Kim Y, Choi JW, Lee JH, Kim YS. Expression of lactate/H(+) symporters MCT1 and MCT4 and their chaperone CD147 predicts tumor progression in clear cell renal cell carcinoma: immunohistochemical and The Cancer Genome Atlas data analyses. *Hum Pathol* 2015;46:104–12.
- Doyen J, Trastour C, Ettore F, Peyrottes I, Toussant N, Gal J, et al. Expression of the hypoxia-inducible monocarboxylate transporter MCT4 is increased in triple negative breast cancer and correlates independently with clinical outcome. *Biochem Biophys Res Commun* 2014;451:54–61.
- Fisel P, Kruck S, Winter S, Bedke J, Hennenlotter J, Nies AT, et al. DNA methylation of the SLC16A3 promoter regulates expression of the human lactate transporter MCT4 in renal cancer with consequences for clinical outcome. *Clin Cancer Res* 2013;19:5170–81.
- Gotanda Y, Akagi Y, Kawahara A, Kinugasa T, Yoshida T, Ryu Y, et al. Expression of monocarboxylate transporter (MCT)-4 in colorectal cancer and its role: MCT4 contributes to the growth of colorectal cancer with vascular endothelial growth factor. *Anticancer Res* 2013;33:2941–7.
- Pinheiro C, Sousa B, Albergaria A, Paredes J, Dufloth R, Vieira D, et al. GLUT1 and CAIX expression profiles in breast cancer correlate with adverse prognostic factors and MCT1 overexpression. *Histol Histopathol* 2011;26:1279–86.
- Hemdan T, Malmstrom PU, Jahnsen S, Segersten U. Emmprin expression predicts response and survival following cisplatin-containing chemotherapy for bladder cancer: a validation study. *J Urol* 2015;194:1575–81.
- Szubert S, Szperek D, Moszynski R, Nowicki M, Frankowski A, Sajdak S, et al. Extracellular matrix metalloproteinase inducer (EMMPRIN) expression correlates positively with active angiogenesis and negatively with basic fibroblast growth factor expression in epithelial ovarian cancer. *J Cancer Res Clin Oncol* 2014;140:361–9.
- Zheng D, Zhu X, Ding X, Zhu X, Yin Y, Li G. Sensitive detection of CD147/EMMPRIN and its expression on cancer cells with electrochemical technique. *Talanta* 2013;105:187–91.
- Zhu S, Chu D, Zhang Y, Wang X, Gong L, Han X, et al. EMMPRIN/CD147 expression is associated with disease-free survival of patients with colorectal cancer. *Med Oncol* 2013;30:369.
- Hao J, Chen H, Madigan MC, Cozzi PJ, Beretov J, Xiao W, et al. Co-expression of CD147 (EMMPRIN), CD44v3-10, MDR1 and monocarboxylate transporters is associated with prostate cancer drug resistance and progression. *Br J Cancer* 2010;103:1008–18.
- Fisel P, Schaeffeler E, Schwab M. Clinical and functional relevance of the monocarboxylate transporter family in disease pathophysiology and drug therapy. *Clin Transl Sci* 2018;11:352–64.
- Chen T, Zhu J. Evaluation of EMMPRIN and MMP-2 in the prognosis of primary cutaneous malignant melanoma. *Med Oncol* 2009;27:1185–91.
- Sienel W, Polzer B, Elshawi K, Lindner M, Morresi-Hauf A, Vay C, et al. Cellular localization of EMMPRIN predicts prognosis of patients with operable lung adenocarcinoma independent from MMP-2 and MMP-9. *Mod Pathol* 2008;21:1130–8.
- Eilertsen M, Andersen S, Al-Saad S, Kiselev Y, Donnem T, Stenvold H, et al. Monocarboxylate transporters 1–4 in NSCLC: MCT1 is an independent prognostic marker for survival. *PLoS One* 2014;9:e105038.
- Fisel P, Stuhler V, Bedke J, Winter S, Rausch S, Hennenlotter J, et al. MCT4 surpasses the prognostic relevance of the ancillary protein CD147 in clear cell renal cell carcinoma. *Oncotarget* 2015;6:30615–27.
- Morais-Santos F, Granja S, Miranda-Goncalves V, Moreira AH, Queiros S, Vilaca JL, et al. Targeting lactate transport suppresses *in vivo* breast tumour growth. *Oncotarget* 2015;6:19177–89.
- Gerlinger M, Santos CR, Spencer-Dene B, Martinez P, Endesfelder D, Burrell RA, et al. Genome-wide RNA interference analysis of renal carcinoma survival regulators identifies MCT4 as a Warburg effect metabolic target. *J Pathol* 2012;227:146–56.
- Baek G, Tse YF, Hu Z, Cox D, Buboltz N, McCue P, et al. MCT4 defines a glycolytic subtype of pancreatic cancer with poor prognosis and unique metabolic dependencies. *Cell Rep* 2014;9:2233–49.
- Afonso J, Santos LL, Miranda-Goncalves V, Morais A, Amaro T, Longatto-Filho A, et al. CD147 and MCT1-potential partners in bladder cancer aggressiveness and cisplatin resistance. *Mol Carcinog* 2015;54:1451–66.
- Shi H, Jiang H, Wang L, Cao Y, Liu P, Xu X, et al. Overexpression of monocarboxylate anion transporter 1 and 4 in T24-induced cancer-

- associated fibroblasts regulates the progression of bladder cancer cells in a 3D microfluidic device. *Cell Cycle* 2015;14:3058–65.
27. Choi JW, Kim Y, Lee JH, Kim YS. Prognostic significance of lactate/proton symporters MCT1, MCT4, and their chaperone CD147 expressions in urothelial carcinoma of the bladder. *Urology* 2014;84:245.
 28. Seiler R, Ashab HA, Erho N, van Rhijn BW, Winters B, Douglas J, et al. Impact of molecular subtypes in muscle-invasive bladder cancer on predicting response and survival after neoadjuvant chemotherapy. *Eur Urol* 2017;72:544–54.
 29. Gust KM, McConkey DJ, Awrey S, Hegarty PK, Qing J, Bondaruk J, et al. Fibroblast growth factor receptor 3 is a rational therapeutic target in bladder cancer. *Mol Cancer Ther* 2013;12:1245–54.
 30. Choi SY, Xue H, Wu R, Fazli L, Lin D, Collins CC, et al. The MCT4 gene: a novel, potential target for therapy of advanced prostate cancer. *Clin Cancer Res* 2016;22:2721–33.
 31. Jager W, Moskalev I, Janssen C, Hayashi T, Awrey S, Gust KM, et al. Ultrasound-guided intramural inoculation of orthotopic bladder cancer xenografts: a novel high-precision approach. *PLoS One* 2013;8:e59536.
 32. Robertson AG, Kim J, Al-Ahmadie H, Bellmunt J, Guo G, Cherniack AD, et al. Comprehensive molecular characterization of muscle-invasive bladder cancer. *Cell* 2017;171:540–56.
 33. Ullah MS, Davies AJ, Halestrap AP. The plasma membrane lactate transporter MCT4, but not MCT1, is up-regulated by hypoxia through a HIF-1alpha-dependent mechanism. *J Biol Chem* 2006;281:9030–7.
 34. Sousa B, Ribeiro AS, Nobre AR, Lopes N, Martins D, Pinheiro C, et al. The basal epithelial marker P-cadherin associates with breast cancer cell populations harboring a glycolytic and acid-resistant phenotype. *BMC Cancer* 2014;14:734.
 35. Iorio F, Knijnenburg TA, Vis DJ, Bignell GR, Menden MP, Schubert M, et al. A landscape of pharmacogenomic interactions in cancer. *Cell* 2016;166:740–54.
 36. Parks SK, Chiche J, Pouyssegur J. Disrupting proton dynamics and energy metabolism for cancer therapy. *Nat Rev Cancer* 2013;13:611–23.
 37. Pouyssegur J, Sardet C, Franchi A, L'Allemain G, Paris S. A specific mutation abolishing Na⁺/H⁺ antiport activity in hamster fibroblasts precludes growth at neutral and acidic pH. *Proc Natl Acad Sci U S A* 1984;81:4833–7.
 38. Lou Y, McDonald PC, Oloumi A, Chia S, Ostlund C, Ahmadi A, et al. Targeting tumor hypoxia: suppression of breast tumor growth and metastasis by novel carbonic anhydrase IX inhibitors. *Cancer Res* 2011;71:3364–76.
 39. Becker HM, Deitmer JW. Nonenzymatic proton handling by carbonic anhydrase II during H⁺-lactate cotransport via monocarboxylate transporter 1. *J Biol Chem* 2008;283:21655–67.
 40. Baenke F, Dubuis S, Brault C, Weigelt B, Dankworth B, Griffiths B, et al. Functional screening identifies MCT4 as a key regulator of breast cancer cell metabolism and survival. *J Pathol* 2015;237:152–65.